Route towards cylindrical cloaking at visible frequencies using an optimization algorithm

Andreas Rottler,[1,*] Benjamin Krüger,[2] Detlef Heitmann,[1] Daniela Pfannkuche,[2] and Stefan Mendach[1]

[1]*Institut für Angewandte Physik und Mikrostrukturforschungszentrum, Universität Hamburg, Jungiusstrasse 11, D-20355 Hamburg, Germany*

[2]*I. Institut für Theoretische Physik, Universität Hamburg, Jungiusstrasse 9, D-20355 Hamburg, Germany*

(Received 24 August 2012; published 19 December 2012)

We derive a model based on the Maxwell-Garnett effective-medium theory that describes a cylindrical cloaking shell composed of metal rods which are radially aligned in a dielectric host medium. We propose and demonstrate a minimization algorithm that calculates for given material parameters the optimal geometrical parameters of the cloaking shell such that its effective optical parameters fit the best to the required permittivity distribution for cylindrical cloaking. By means of sophisticated full-wave simulations we find that a cylindrical cloak with good performance using silver as the metal can be designed with our algorithm for wavelengths in the red part of the visible spectrum (623 nm $< \lambda <$ 773 nm). We also present a full-wave simulation of such a cloak at an exemplary wavelength of $\lambda = 729$ nm ($\hbar\omega = 1.7$ eV) which indicates that our model is useful to find design rules of cloaks with good cloaking performance. Our calculations investigate a structure that is easy to fabricate using standard preparation techniques and therefore pave the way to a realization of guiding light around an object at visible frequencies, thus rendering it invisible.

DOI: 10.1103/PhysRevB.86.245120 PACS number(s): 81.05.Xj, 78.67.Pt, 42.15.Eq, 41.20.−q

I. INTRODUCTION

Besides concepts like imaging beyond the diffraction limit[1–5] or negative refraction,[6–10] invisibility cloaking is one intriguing capability of metamaterials. This concept could lead on the one hand to the long human dream of rendering things invisible, on the other hand also applications like a cloaking material covering a near-field scanning optical microscope tip, thus improving the sensing mechanism, are possible.[11–14]

Utilizing the mathematical concept of transformation optics,[15–17] a cylindrical cloaking device was proposed and has been eventually demonstrated in the microwave regime.[18] An alternative concept for cloaking at visible frequencies is the carpet cloak which hides a perturbation on a flat reflecting plane, i.e., an object can be hidden underneath this perturbation.[19–25] Smolyaninov and co-workers worked in the direction of using tapered waveguides, emulating the required anisotropic permittivity and permeability distribution for cloaking.[26] For the realization of cylindrical cloaks similar to that in Ref. 18 working at visible frequencies, there exist some theoretical concepts, e.g., by using metal-dielectric composites.[27–30] These proposals are, however, quite difficult to implement: For example, in Ref. 27 elongated metal wires with subwavelength dimensions have to be radially orientated in a host medium, whereas in Ref. 29 spherical metal particles are used, however their distances have to be precisely controlled.

In this paper we demonstrate that a cylindrical cloaking device operating in the red part of the visible spectrum can be fabricated by metal rods that are incorporated into a dielectric host material (as recommended in Ref. 31). The design is chosen such that it could be fabricated by using standard preparation techniques (for a realization of stacked nanowires with tailored parameters using current lithographic methods see, for example, Ref. 32). We propose and utilize an optimization algorithm that calculates the geometrical parameters of a cylindrical cloak made of metal rods radially aligned in a dielectric host medium for a given frequency and material properties. We show that a set of parameters for an invisibility cloak made of silver and poly methyl methacrylate (PMMA) can be found for wavelength λ in the visible spectrum between $\lambda = 623$ nm (energy $\hbar\omega = 1.99$ eV) and $\lambda = 773$ nm ($\hbar\omega = 1.60$ eV). This wavelength range is determined by the constraints on the shape of the metal inclusions. The working principle of our approach is demonstrated for an exemplary wavelength of $\lambda = 729$ nm ($\hbar\omega = 1.7$ eV). We validate the applicability of our model by means of full-wave simulations of the realistic rod arrangement demonstrating that our model is useful to find design rules of cloaks with good cloaking performance.

The paper is organized as follows: In Sec. II we derive and present the minimization algorithm that is used to calculate the optimal geometrical parameters of the cloaking shell. In Sec. III we exemplarily demonstrate the working principle of the algorithm at a wavelength $\lambda = 729$ nm ($\hbar\omega = 1.7$ eV). With full-wave simulations of the realistic structure we confirm that a cloak with good performance can be designed using our model. We further validate that the major reason for the nonoptimal performance is damping due to absorption in the metal. A conclusion is given in Sec. IV.

II. MODEL

In the permittivity and permeability tensors that are obtained from the standard coordinate transformation for cylindrical cloaking, each component on the diagonal depends on the radial coordinate.[15] Therefore, a reduced set of parameters is usually used to simplify an experimental realization.[27,33] This reduced parameter set reads

$$\mu_z = 1, \quad \epsilon_\theta = \left(\frac{b}{b-a}\right)^2, \quad \epsilon_r(r) = \left(\frac{b}{b-a}\right)^2 \left(\frac{r-a}{r}\right)^2, \tag{1}$$

where μ_z is the permeability component in the z direction and ϵ_θ and ϵ_r are the azimuthal and radial permittivity component, respectively. All other tensor components can be chosen arbitrarily. We remark that in this case the incident wave has

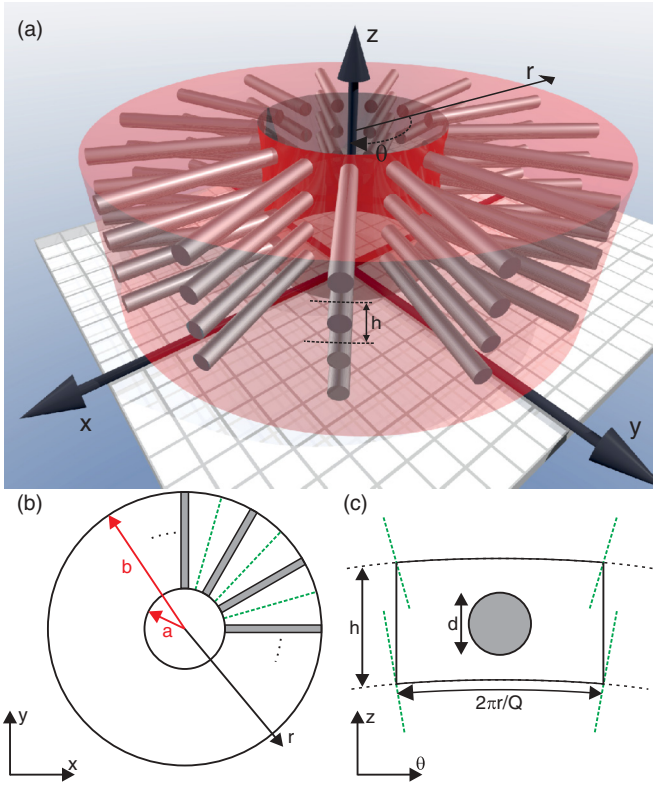

FIG. 1. (Color online) (a) The discussed cylindrical cloaking shell consists of metal rods that are radially aligned in a dielectric host medium. The vertical distance of the rods is denoted by h. (b) Scheme of the cloak with inner and outer radius a and b, respectively. (c) Side view of one segment at a radial position r with $a \leqslant r \leqslant b$.

to be TM polarized, i.e., the magnetic field vector points along the z direction. Furthermore, scattering of the cloaking shell occurs, due to an inherent impedance mismatch at the outer perimeter of the cloaking shell.[27] For a reduced parameter set for TM waves the magnetic dependence is entirely removed, that is, it has no influence on the magnetic field. Also, ϵ_θ has a constant value and ϵ_r depends only on the radial coordinate with values between 0 and 1.

Figures 1(a)–1(c) sketch the investigated structure. The inner and outer cloak radius are denoted as a and b, respectively, i.e., $a < b$. Metal cylinders of length $b - a$ and diameter d are radially aligned in the cloaking shell, with equal distance in the azimuthal direction. The host medium is assumed to be a dielectric with constant permittivity ϵ_h. The number of cylinders along a 2π rotation is given by the integer number Q and the distance of adjacent rods in the z direction is denoted by h. The effective response of the metal-dielectric composite can be modeled within the Maxwell-Garnett effective-medium approximation.[34,35] In this model the effective permittivity in the r direction ($\epsilon_{r,\mathrm{MG}}$) and the θ direction ($\epsilon_{\theta,\mathrm{MG}}$) can be written as[36]

$$\epsilon_{\theta,\mathrm{MG}} = \epsilon_\mathrm{h}\left(1 + \frac{2f}{(f-1)(L_r-1) - 2s}\right), \tag{2}$$

$$\epsilon_{r,\mathrm{MG}} = \epsilon_\mathrm{h}\left(1 - \frac{f}{s - L_r(1-f)}\right). \tag{3}$$

In these formulas s is a dimensionless quantity that depends on the permittivities of the metal [$\epsilon_\mathrm{m}(\omega)$] and dielectric ($\epsilon_\mathrm{h}$):

$$s = s(\omega) = \frac{1}{1 - \frac{\epsilon_\mathrm{m}(\omega)}{\epsilon_\mathrm{h}}}. \tag{4}$$

L_r is the depolarization factor along the axis of the rod. Due to the specific symmetry of the rods, the depolarization factors along the z and the azimuthal direction are equal and we denote them by L_t. The depolarization factors satisfy the sum rule $L_r + 2L_t = 1$. For a prolate ellipsoid the depolarization factors in the different directions can be calculated in a closed form (see, e.g., Ref. 37). This is however not possible for a cylindrical rod, but if the rods are very long and thin, then L_r is very close to zero and L_t approaches $1/2$. In this case L_r can be approximated by the following equation:[38,39]

$$L_r = \left(\frac{d}{(b-a)}\right)^2 \ln\left(\frac{(b-a)}{d}\right). \tag{5}$$

The quantity f denotes the metal volume fraction (or "filling fraction"). It becomes clear from Fig. 1(b) that the radial alignment of the rods leads to a decreasing f from the inner perimeter of the cloaking shell to the outer one, i.e., $f = f(r)$. At a position r with $a \leqslant r \leqslant b$ the metal filling fraction can be calculated as [cf. Fig. 1(c)]

$$f(r) = \frac{\pi(d/2)^2}{2\pi r/Q h} = \frac{d^2 Q}{8rh}. \tag{6}$$

The criterion that the metal-dielectric composite works as a cylindrical cloaking device is the following: Most favorable, the real parts of the radial and azimuthal permittivities calculated with the Maxwell-Garnett formula [Eqs. (2) and (3)] equal the permittivities required for cloaking [Eqs. (1)] throughout the cloak. In our computational model it is necessary to discretize this problem into N steps. We chose $N = 1000$, finding that a larger N did not lead to different solutions. The problem can then be formulated as

$$\epsilon_\theta \stackrel{!}{=} \mathrm{Re}\left(\epsilon^j_{\theta,\mathrm{MG}}\right), \tag{7}$$

$$\epsilon_r\left[a + \frac{2j-1}{2}\left(\frac{b-a}{N}\right)\right] \stackrel{!}{=} \mathrm{Re}\left(\epsilon^j_{r,\mathrm{MG}}\right), \tag{8}$$

with $j = 1, \ldots, N$. The exact fulfillment of both equations for each j cannot be achieved. Especially $\mathrm{Re}(\epsilon^j_{\theta,\mathrm{MG}})$ will not match the constant value $\epsilon_\theta = b^2/(b-a)^2$ for each j. A strategy to deal with this problem is the definition of a minimization problem that can be numerically solved. For that purpose we define the radial and azimuthal deviations $s_{\theta,j}$ and $s_{r,j}$ as

$$s_{\theta,j} = \left|\epsilon_\theta - \mathrm{Re}\left(\epsilon^j_{\theta,\mathrm{MG}}\right)\right|^2, \tag{9}$$

$$s_{r,j} = \left|\epsilon_r\left[a + \frac{2j-1}{2}\left(\frac{b-a}{N}\right)\right] - \mathrm{Re}\left(\epsilon^j_{r,\mathrm{MG}}\right)\right|^2. \tag{10}$$

We would like to remark here that we found from our cloaking simulations that it is more important to find a good coincidence of the radial permittivity, rather than the azimuthal one. We therefore introduce a weighting factor q ($1 < q \in \mathbb{R}$) to address this requirement. In that sense the minimization

problem can be formulated as follows:

$$\text{minimize:} \quad S = \sum_{j=1}^{N} (s_{\theta,j} + q^2 s_{r,j}). \tag{11}$$

We utilize a Levenberg-Marquardt algorithm[40,41] to find the optimal solution for a given frequency ω and given material parameters $\epsilon_m(\omega)$ and ϵ_h. The variables in the algorithm are the dimensionless quantities $p_0 := b/a$, $p_1 := L_r$, and $p_2 := d^2Q/(8ha) \equiv f(r) \cdot r/a$. Specifying an inner radius for the cloak, one can calculate the outer radius from p_0. With this information and p_1 a metal rod diameter d can be calculated by inverting Eq. (5). From p_2, which is a quantity representing the metal filling fraction, the ratio Q/h, i.e., total number of cylinders divided by vertical distance, can be derived. From Q/h, the vertical rod distance h can be calculated for a given Q. At first glance, one could guess that there are no constraints on the number Q, as long as it does not lead to an overlap of adjacent metal rods in the azimuthal and also in the z direction. It has to be recognized that the Maxwell-Garnett effective-medium approximation considers the metal inclusions as point dipoles. Therefore, it does not take coupling effects between the rods into account. However, Pitarke *et al.* calculated for a periodic array of long and thin metal cylinders that the Maxwell-Garnett model delivers good results when the distance between the axis of neighboring rods is twice the diameter of the rods or larger.[42] This is also supported by calculations on metal nanoparticles performed in Ref. 29. Consequently, in calculating Q and h one should pay attention that the relations $h/d > 2$ and $2\pi a/(Qd) > 2$ are fulfilled.

An additional constraint is set for the depolarization factor L_r. The validity of Eq. (5) requires that the length of the metal rod is considerably larger than the diameter, such that L_r is very close to zero. For prolate ellipsoidal particles this is the case if the length-to-diameter ratio $(b-a)/d$ is approximately 10 or larger. Otherwise, if $(b-a)/d < 10$, L_r increases rapidly (see, e.g., Ref. 43). If we assume a length-to-diameter ratio of larger than 10, we can derive from Eq. (5) that the condition $L_r < 0.023$ should be satisfied.

III. RESULTS AND DISCUSSION

In this section we describe the results that we obtain from the minimization algorithm for visible frequencies. As the dielectric host medium we chose PMMA, which was modeled with a constant permittivity of $\epsilon_h = 2.25$ and we assume $\mathrm{Im}(\epsilon_h) = 0$. In the following we assume silver as the metal with complex permittivity values $\epsilon_m(\omega)$ as a linear interpolation on experimental data taken from Ref. 44. Calculations have been performed for wavelengths in the visible spectrum; in the following graphs we concentrate on the spectral region between $\lambda = 550$ nm ($\hbar\omega = 2.25$ eV) and $\lambda = 770$ nm ($\hbar\omega = 1.61$ eV). Figures 2(a)–2(c) show the values for the quantities p_0, p_1, and p_2 for the optimal solution of Eq. (11). The weighting factor q, quantifying the tradeoff between $s_{\theta,j}$ and $s_{r,j}$, was chosen as $q = 5$ (solid lines) and $q = 3$ (dashed lines). Figure 2(d) displays S which denotes the sum of squared residuals and is therefore a number that quantifies the agreement of the Maxwell-Garnett theory with the reduced

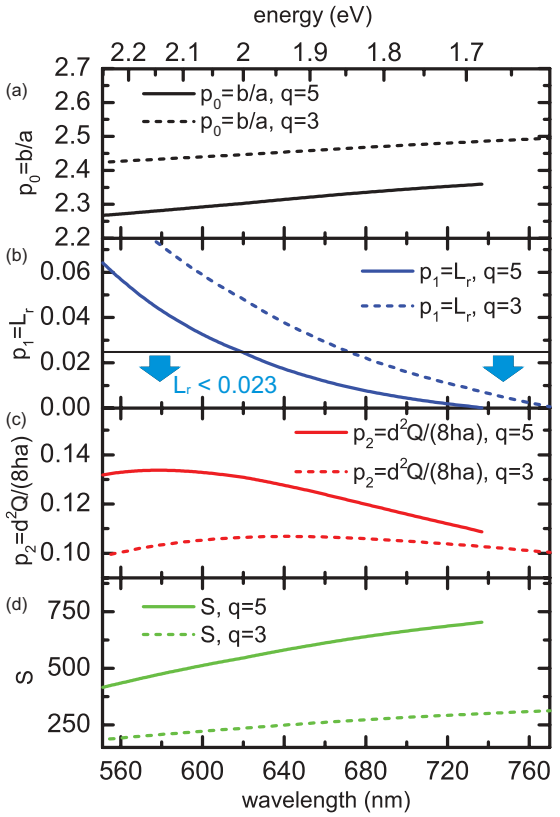

FIG. 2. (Color online) For the optimal solution of Eq. (11) we displayed (a) the quantity $p_0 = b/a$, (b) the quantity $p_1 = L_r$, and (c) the quantity $p_2 = d^2Q/(8ha)$. Panel (d) depicts S, the sum of squared residuals. Solid lines depict the results for a weighting factor $q = 5$, while the dashed lines indicate these quantities for $q = 3$.

parameter set [cf. Eq. (11)]. It is found that p_0, the ratio of outer and inner radius, lies for both $q = 3$ and $q = 5$ between 2.27 and 2.49 which is of comparable magnitude to, e.g., b/a of the microwave cylindrical cloak of Schurig *et al.*, which was determined there as 2.17 (Ref. 18). p_1 decreases with increasing wavelength, while S has obviously larger values for $q = 5$ than for $q = 3$. p_1, the depolarization factor, has for $q = 5$ a value of 0.023 at $\lambda = 623$ nm (energy $\hbar\omega = 1.99$ eV). For shorter wavelengths a converging set of parameters p_0, p_1, and p_2 can only be found if $p_1 = L_r > 0.023$ would be allowed. On the other hand L_r turns negative for wavelengths larger than $\lambda = 736$ nm (energy $\hbar\omega = 1.68$ eV), thus marking the upper wavelength limit for the $q = 5$ case. For $q = 3$, however, we find that $p_1 = L_r < 0.023$ for 677 nm $< \lambda <$ 773 nm, i.e., suitable parameters of p_0, p_1, and p_2 can be found for larger wavelengths up to the end of the visible part of the spectrum. It has to be noted that also for $q > 5$ suitable values of p_0, p_1, and p_2 can be found at certain frequencies in the red part of the spectrum. We remark that cloak designs for shorter wavelengths can be obtained by using a metal with larger plasma frequency, e.g., aluminum.

In Fig. 3(a) we display the reduced parameter permittivities ϵ_θ, $\epsilon_r(r)$ [Eq. (1)] and the obtained real and imaginary part of the Maxwell-Garnett permittivities $\epsilon_{\theta,\mathrm{MG}}$, $\epsilon_{r,\mathrm{MG}}$ [Eqs. (2) and (3)] at a wavelength of $\lambda = 729$ nm (energy $\hbar\omega = 1.7$ eV) for $q = 5$. The obtained values of p_0, p_1, and p_2 from the

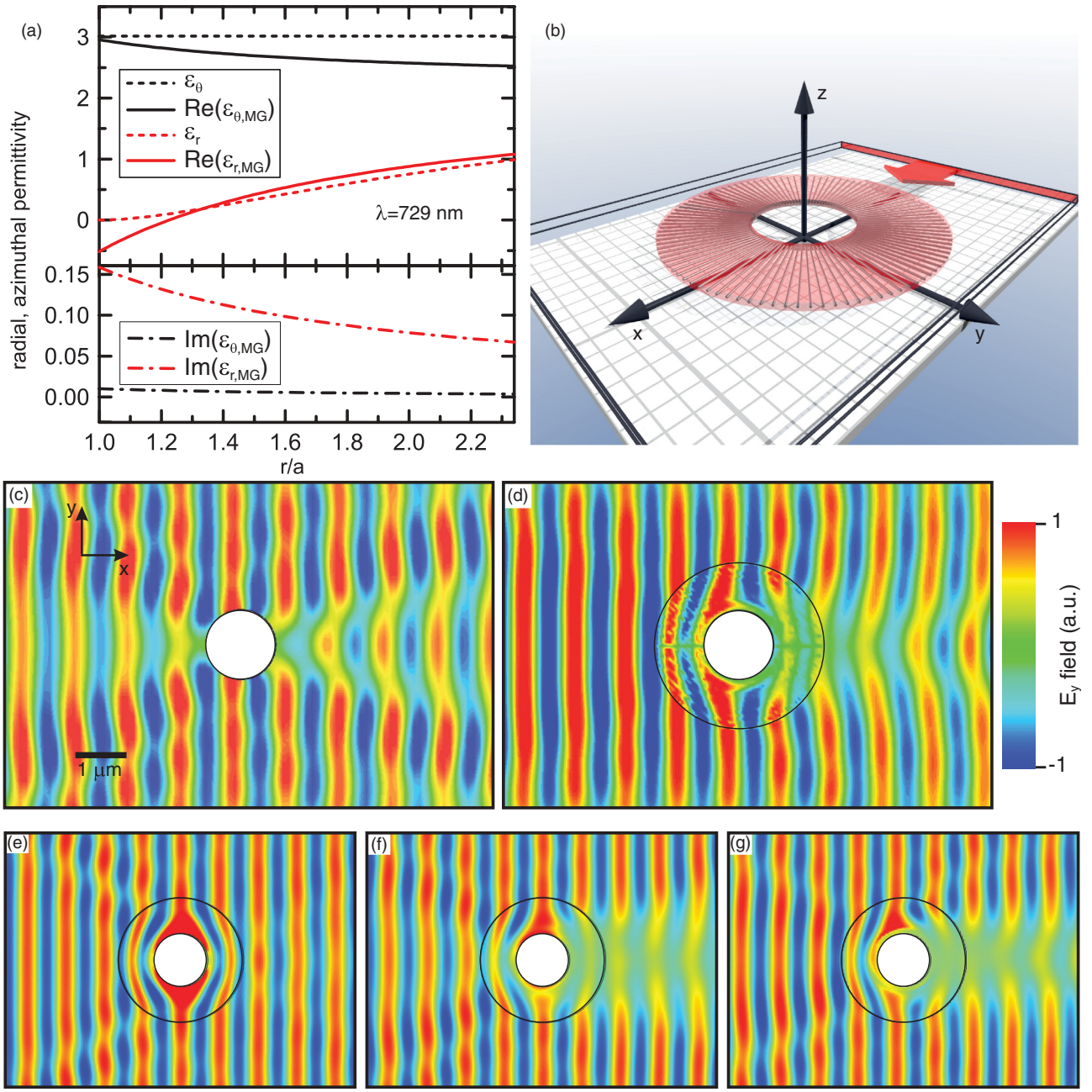

FIG. 3. (Color online) (a) Comparison of the reduced parameter permittivities [$\epsilon_r(r), \epsilon_\theta$, cf. Eq. (1)] and the real parts of the Maxwell-Garnett permittivities [$\mathrm{Re}(\epsilon_{r,\mathrm{MG}})$, $\mathrm{Re}(\epsilon_{\theta,\mathrm{MG}})$, cf. Eqs. (2) and (3)] for a wavelength of $\lambda = 729$ nm ($\hbar\omega = 1.7$ eV) and the corresponding values of $p_0 = 2.36$, $p_1 = 9.33 \times 10^{-4}$, and $p_2 = 0.11$. The lower part depicts the imaginary parts of the Maxwell-Garnett permittivities, $\mathrm{Im}(\epsilon_{r,\mathrm{MG}})$ and $\mathrm{Im}(\epsilon_{\theta,\mathrm{MG}})$, respectively. (b) Sketch of the simulation setup of the cloaking structure. (c) The pattern of the component E_y of the electric field in the x-y plane for a bare perfect electric conductor cylinder. (d) The pattern of the component E_y of the electric field in the x-y plane with the cloak. (e) Simulation with a cloaking shell obeying the reduced material parameters [Eq. (1)]. (f) Same as in (e) but with an assumed loss tangent of 0.1 in the cloaking shell, i.e., we added a term $0.1i$ to ϵ_θ and $\epsilon_r(r)$ in Eq. (1). Panel (g) is a simulation similar to (e) and (f) but with the complex Maxwell-Garnett permittivities $\epsilon_{r,\mathrm{MG}}$ and $\epsilon_{\theta,\mathrm{MG}}$. Movies showing the time development of the field in (c) and (d) are available via the Supplemental Material (Ref. 45).

algorithm at this wavelength are $p_0 = 2.36$, $p_1 = 9.33 \times 10^{-4}$ and $p_2 = 0.11$ [cf. Figs. 2(a)–2(c)]. For the value of $\mathrm{Re}(\epsilon_{\theta,\mathrm{MG}})$ it can be seen that there is quite a good coincidence with ϵ_θ at the inner perimeter of the cloaking shell. To the outer perimeter the deviation increases with a maximum discrepancy of 16%. Concerning $\mathrm{Re}(\epsilon_{r,\mathrm{MG}})$ there is a good agreement with $\epsilon_r(r)$ at the outer parts of the cloak with $\mathrm{Re}(\epsilon_{r,\mathrm{MG}})$ being slightly larger than $\epsilon_r(r)$ for $r/a > 1.32$. For values of $r/a < 1.32$, $\mathrm{Re}(\epsilon_{r,\mathrm{MG}})$ drops below $\epsilon_r(r)$, becoming negative for $r/a < 1.23$. It reaches it maximum negative value of -0.5 at the inner radius of the shell (where $r/a = 1.0$). We find that $\mathrm{Re}(\epsilon_{r,\mathrm{MG}})$ becomes negative near the inner perimeter of the cloaking shell which is typical for all investigated wavelengths. However, it turned out that both this and the deviations in $\mathrm{Re}(\epsilon_{\theta,\mathrm{MG}})$

are not a major drawback to the cloaking performance, as discussed below. Concerning the imaginary parts we find that $\mathrm{Im}(\epsilon_{\theta,\mathrm{MG}})$ is very close to zero throughout the cloaking shell, while $\mathrm{Im}(\epsilon_{r,\mathrm{MG}})$ drops from 0.16 to 0.07 from the inner to the outer perimeter. This declining behavior is expected due to the decreasing metal-filling fraction. The loss tangent of approximately 0.1 is in very good agreement with the value from previous publications on cylindrical cloaks made of metal inclusions which also calculated an effective imaginary part of the cloaking shell of about 0.1.[27,29]

To verify that our model is applicable to find designs of an invisibility cloak we performed a full-wave simulation of the realistic structure as shown in Fig. 1(a), utilizing the commercial finite-integration-technique software CST microwave studio.[46] The permittivity of the silver rods is again a linear interpolation on experimental data from the Palik book (Ref. 44). We exemplarily show here the investigation of a cloak performing at a wavelength of $\lambda = 729$ nm ($\hbar\omega = 1.7$ eV). We chose an inner radius of the shell of $a = 0.5\ \mu$m, leading with $p_0 = 2.36$ to an outer radius of $b = 1.18\ \mu$m. The length of the metal rods is therefore $b - a = 0.70\ \mu$m. From the depolarization factor $L_r = p_1 = 9.33 \times 10^{-4}$ we derived a diameter of the rods of $d = 0.01\ \mu$m. The value of $p_2 = 0.11$ leads to a ratio Q/h of $Q/h = 4325\ \mu\mathrm{m}^{-1}$. We fix Q, the azimuthal number of rods, to $Q = 100$ (note that this choice is at first glance random, other values of Q are principally possible) and obtain $h = 0.023\ \mu$m. Both values for Q and h are in accordance with the requirements set by Ref. 42, since $h/d > 2$ and $2\pi a/(Qd) > 2$. We remark that all dimensions are scalable, i.e., if we would increase the inner radius of the shell by a factor of 2, all other geometrical dimensions have to be two times larger. This is, in principle, no problem. However, we find that the cloaking effect is considerably diminished when the diameter of the rods exceeds 20 nm. This could be attributed to the excitation of surface plasmon polaritons on the metal surface. Figure 3(b) shows a sketch of the simulation setup. The vertical periodicity of the cloak was modeled using periodic boundary conditions in z direction, i.e., in Fig. 3(b) only one slice of the cloaking shell is displayed. The radial alignment of the 100 metal rods inside the shell is clearly visible. Inside the cloaking shell we placed a perfect electric conductor (PEC) cylinder with radius $a = 0.5\ \mu$m. A plane wave of wavelength $\lambda = 729$ nm ($\hbar\omega = 1.7$ eV) is excited at the rear boundary, propagating in positive x direction. In Fig. 3(d) the component E_y of the electric field in the x-y plane is displayed. It can be seen that the cloaking effect is not perfect, however the scattering is considerably lower than that of a bare PEC cylinder of radius a [Fig. 3(c); see also the movies in the Supplemental Material of this paper[45]]. Moreover, it can be seen that the field inside the cloaking shell forms the characteristic cylindrical cloaking pattern of field lines bending around the object [cf., e.g., Fig. 3(e)]. This is an evidence that the investigated cloak with the metal rods does indeed provide the required permittivity distribution that is needed for cylindrical cloaking.

There are two main reasons why the cloaking effect is diminished: (i) The use of the reduced parameter set instead of the ideal permittivity and permeability set leads to inherent scattering and therefore to a disturbance of the fields in the cloak and (ii) the finite imaginary part of the metal permittivity leads to losses which are the reason why the field is damped inside the cloak. To clarify their influence on the cloaking effect we performed two additional simulations using the finite-element solver COMSOL Multiphysics.[47] In Fig. 3(e) a corresponding two-dimensional simulation of a cloak with the reduced parameters [Eq. (1)] is shown. The plane wave gets bent around the inner core with the field showing the characteristic pattern inside the cloaking shell. Material loss has been set to zero in this simulation and only minor reflections are observed, due to the inherent scattering. To examine the influence of the ohmic losses in the metal compound we performed the same simulation as in Fig. 3(e), but now take the material losses into account. We already mentioned that the average loss tangent in the cloaking shell was determined to be 0.1. Therefore, Fig. 3(f) shows the simulation where we assume a loss tangent of 0.1 in the shell, i.e., we added a term $0.1i$ to ϵ_θ and $\epsilon_r(r)$ in Eq. (1). This leads to a field pattern behind the cloak which is very much comparable to that in Fig. 3(d), where the metal-rod structure has been simulated. The damping still leads to a shadow behind the object. We can therefore conclude that the metal loss is the main factor that needs to be overcome to obtain a better cloaking performance. The reduction of losses is one important field in metamaterial research that many groups work on (see, e.g., Refs. 48–52).

In Fig. 3(g) we performed a simulation similar to that in Figs. 3(e) and 3(f), but with the complex Maxwell-Garnett permittivities $\epsilon_{r,\mathrm{MG}}$ and $\epsilon_{\theta,\mathrm{MG}}$ in the cloaking shell [cf. Fig. 3(a)]. The field pattern is again very similar to the full-wave simulation of the realistic structure [Fig. 3(d)]. Thus, this is an evidence that the Maxwell-Garnett effective-medium theory is indeed applicable to describe a cylindrical cloaking device made of metal rods embedded into a dielectric host material.

IV. CONCLUSION

In conclusion we have introduced a theoretical model based on the Maxwell-Garnett effective-medium theory and a minimization algorithm that calculates the optimal geometrical dimensions of an invisibility cloak, which is made of metal rods embedded in a dielectric host material and works at visible wavelengths. We show that an invisibility cloak with good performance can be designed for wavelengths in the red part of the visible spectrum between $\lambda = 623$ nm (energy $\hbar\omega = 1.99$ eV) and $\lambda = 773$ nm (energy $\hbar\omega = 1.60$ eV). We also present a full-wave simulation of such a cloak at an exemplary wavelength of $\lambda = 729$ nm ($\hbar\omega = 1.7$ eV) which indicates that our model is useful to find design rules of cloaks with good cloaking performance. It is found that the major reason degrading the cloaking performance is damping, due to the metal compound.

ACKNOWLEDGMENTS

We gratefully acknowledge support of the Deutsche Forschungsgemeinschaft via the Graduiertenkolleg 1286 "Functional Metal-Semiconductor Hybrid Systems" as well as SFB 668, and the City of Hamburg via the Cluster of Excellence Nano-Spintronics.

*arottler@physnet.uni-hamburg.de

[1] J. B. Pendry, Phys. Rev. Lett. **85**, 3966 (2000).
[2] N. Fang, H. Lee, C. Sun, and X. Zhang, Science **308**, 534 (2005).
[3] Z. Liu, H. Lee, Y. Xiong, C. Sun, and X. Zhang, Science **315**, 1686 (2007).
[4] S. Schwaiger, M. Bröll, A. Krohn, A. Stemmann, C. Heyn, Y. Stark, D. Stickler, D. Heitmann, and S. Mendach, Phys. Rev. Lett. **102**, 163903 (2009).
[5] S. Schwaiger, A. Rottler, M. Bröll, J. Ehlermann, A. Stemmann, D. Stickler, C. Heyn, D. Heitmann, and S. Mendach, Phys. Rev. B **85**, 235309 (2012).
[6] R. A. Shelby, D. R. Smith, and S. Schultz, Science **292**, 77 (2001).
[7] V. M. Shalaev, W. Cai, U. K. Chettiar, H.-K. Yuan, A. K. Sarychev, V. P. Drachev, and A. V. Kildishev, Opt. Lett. **30**, 3356 (2005).
[8] G. Dolling, C. Enkrich, M. Wegener, C. M. Soukoulis, and S. Linden, Opt. Lett. **31**, 1800 (2006).
[9] J. Valentine, S. Zhang, T. Zentgraf, E. Ulin-Avila, D. A. Genov, G. Bartal, and X. Zhang, Nature (London) **455**, 376 (2008).
[10] A. Rottler, M. Harland, M. Bröll, S. Schwaiger, D. Stickler, A. Stemmann, C. Heyn, D. Heitmann, and S. Mendach, Appl. Phys. Lett. **100**, 151104 (2012).
[11] A. Alù and N. Engheta, Phys. Rev. Lett. **102**, 233901 (2009).
[12] A. Alù and N. Engheta, Phys. Rev. Lett. **105**, 263906 (2010).
[13] F. Bilotti, S. Tricarico, F. Pierini, and L. Vegni, Opt. Lett. **36**, 211 (2011).
[14] X. Chen and G. Uhlmann, Opt. Express **19**, 20518 (2011).
[15] J. B. Pendry, D. Schurig, and D. R. Smith, Science **312**, 1780 (2006), http://www.sciencemag.org/cgi/reprint/312/5781/1780.pdf.
[16] U. Leonhardt, Science **312**, 1777 (2006).
[17] H. Chen, C. T. Chan, and P. Sheng, Nat. Mater. **9**, 387 (2010).
[18] D. Schurig, J. J. Mock, B. J. Justice, S. A. Cummer, J. B. Pendry, A. F. Starr, and D. R. Smith, Science **314**, 977 (2006).
[19] J. Li and J. B. Pendry, Phys. Rev. Lett. **101**, 203901 (2008).
[20] L. H. Gabrielli, J. Cardenas, C. B. Poitras, and M. Lipson, Nat. Photon. **3**, 461 (2009).
[21] J. Valentine, J. Li, T. Zentgraf, G. Bartal, and X. Zhang, Nat. Mater. **8**, 568 (2009).
[22] T. Ergin, N. Stenger, P. Brenner, J. B. Pendry, and M. Wegener, Science **328**, 337 (2010).
[23] T. Ergin, J. Fischer, and M. Wegener, Phys. Rev. Lett. **107**, 173901 (2011).
[24] J. Fischer, T. Ergin, and M. Wegener, Opt. Lett. **36**, 2059 (2011).
[25] M. Gharghi, C. Gladden, T. Zentgraf, Y. Liu, X. Yin, J. Valentine, and X. Zhang, Nano Lett. **11**, 2825 (2011).
[26] I. I. Smolyaninov, V. N. Smolyaninova, A. V. Kildishev, and V. M. Shalaev, Phys. Rev. Lett. **102**, 213901 (2009).
[27] W. Cai, U. K. Chettiar, A. V. Kildishev, and V. M. Shalaev, Nat. Photon. **1**, 224 (2007).
[28] Y. Xie, H. Chen, Y. Xu, L. Zhu, H. Ma, and J.-W. Dong, Plasmonics **6**, 477 (2011).
[29] D. Diedrich, A. Rottler, D. Heitmann, and S. Mendach, New J. Phys. **14**, 053042 (2012).
[30] W. Cai, U. K. Chettiar, A. V. Kildishev, and V. M. Shalaev, Opt. Express **16**, 5444 (2008).
[31] T. Ergin and M. Wegener, Phys. J. **11**, 31 (2012).
[32] Y. Zhao, M. Belkin, and A. Alu, Nat. Commun. **3**, 870 (2012).
[33] S. A. Cummer, B.-I. Popa, D. Schurig, D. R. Smith, and J. Pendry, Phys. Rev. E **74**, 036621 (2006).
[34] J. C. M. Garnett, Philos. Trans. R. Soc. London A **203**, 385 (1904).
[35] A. Sihvola, *Electromagnetic Mixing Formulae and Applications*, edited by IEEE Electromagnetic Waves Series (The Institution of Engineering and Technology, 1999).
[36] Y. Gao, J. P. Huang, and K. W. Yu, J. Appl. Phys. **105**, 124505 (2009).
[37] A. Sihvola, J. Nano. **2007**, 45090 (2007).
[38] S. M. Matitsine, K. M. Hock, L. Liu, Y. B. Gan, A. N. Lagarkov, and K. N. Rozanov, J. Appl. Phys. **94**, 1146 (2003).
[39] M. Koledintseva, R. DuBroff, and R. Schwartz, Prog. Electromagn. Res. **63**, 223 (2006).
[40] K. Levenberg, Q. Appl. Math. **2**, 164 (1944).
[41] D. Marquardt, SIAM J Appl. Math. **11**, 431 (1963).
[42] J. M. Pitarke, F. J. Garcia-Vidal, and J. B. Pendry, Phys. Rev. B **57**, 15261 (1998).
[43] V. Myroshnychenko, J. Rodriguez-Fernandez, I. Pastoriza-Santos, A. M. Funston, C. Novo, P. Mulvaney, L. M. Liz-Marzan, and F. J. Garcia de Abajo, Chem. Soc. Rev. **37**, 1792 (2008).
[44] E. Palik, *Handbook of Optical Constants of Solids* (Academic, New York, 1985).
[45] See Supplemental Material at http://link.aps.org/supplemental/10.1103/PhysRevB.86.245120 for movies of the time development of the field in Figs. 3(c) and 3(d).
[46] CST Microwave Studio, http://www.cst.com/, CST Computer Simulation Technology.
[47] COMSOL Multiphysics, http://www.comsol.com/, COMSOL group.
[48] S. Xiao, V. P. Drachev, A. V. Kildishev, X. Ni, U. K. Chettiar, H.-K. Yuan, and V. M. Shalaev, Nature (London) **466**, 735 (2010).
[49] N. Meinzer, M. Ruther, S. Linden, C. M. Soukoulis, G. Khitrova, J. Hendrickson, J. D. Olitzky, H. M. Gibbs, and M. Wegener, Opt. Express **18**, 24140 (2010).
[50] K. Tanaka, E. Plum, J. Y. Ou, T. Uchino, and N. I. Zheludev, Phys. Rev. Lett. **105**, 227403 (2010).
[51] S. Schwaiger, M. Klingbeil, J. Kerbst, A. Rottler, R. Costa, A. Koitmäe, M. Bröll, C. Heyn, Y. Stark, D. Heitmann, and S. Mendach, Phys. Rev. B **84**, 155325 (2011).
[52] A. Rottler, S. Schwaiger, A. Koitmäe, D. Heitmann, and S. Mendach, J. Opt. Soc. Am. B **28**, 2402 (2011).